Available online at www.sciencedirect.com
SCIENCE DIRECT®
Journal of Sound and Vibration 291 (2006) 395–418
JOURNAL OF SOUND AND VIBRATION
www.elsevier.com/locate/jsvi

Crack induced vibration localization in simplified bladed-disk structures

X. Fang, J. Tang*, E. Jordan, K.D. Murphy

Department of Mechanical Engineering, The University of Connecticut, 191 Auditorium Road, Unit 3139, Storrs, CT 06269, USA

Received 12 October 2004; received in revised form 20 May 2005; accepted 15 June 2005
Available online 25 August 2005

Abstract

In this paper, we study the effect of a crack on the vibratory response of a simplified aero-engine bladed-disk model, which consists of cantilevered beams (blades) coupled with springs (inter-blade internal coupling). Our goal is to obtain qualitative understandings of the unique dynamic behavior of such structure with crack, i.e., the occurrence of vibration localization and its level. A fracture mechanics based approach is employed to evaluate the crack induced stiffness loss on a single beam. By taking advantage of the structural periodicity or near-periodicity, using the U-transformation approach we then develop analytical solutions to the free and forced vibrations of the bladed-disk with a single crack. It is identified that, while the stiffness loss on a single beam could be small and may not cause a significant frequency change, it could lead to the free and forced vibration localization in a periodic structure. The intrinsic relation between the response amplitudes and various system parameters such as internal coupling, crack severity, excitation patterns and number of blades is systematically investigated.

1. Introduction and research overview

Bladed-disk structures designed to be cyclically periodic are widely used in turbomachinery. The dynamic analysis of the bladed-disk structures can be greatly simplified by enforcing periodicity, i.e., assuming that all blades are identical and their associated disk sectors are

*Corresponding author. Tel.: +1 860 486 5911.
E-mail address: jtang@engr.uconn.edu (J. Tang).

0022-460X/$ - see front matter © 2005 Elsevier Ltd. All rights reserved.
doi:10.1016/j.jsv.2005.06.020

symmetric and homogeneous [1]. However, in practice, the cyclic symmetry of these structures is inevitably destroyed by imperfections resulted from manufacturing tolerance or in-service damage. These small blade-to-blade irregularities or deviations are oftentimes referred to as mistuning. Periodic structures with weak internal coupling have demonstrated high sensitivity with respect to such mistuning, which may lead to a well-known phenomenon called vibration localization [1–3]. Many studies have shown that even a small degree of mistuning can have a dramatic effect on the vibratory behavior of periodic structures, i.e., a single blade or a few blades of the mistuned structure may experience vibration response amplitudes and local stresses that are excessively high compared to those of the corresponding nominally tuned structure [3].

To date, a significant number of studies [4–10] have focused on the underlying mechanism of vibration localization in bladed-disks. Although these studies have led to some general conclusions, most of them deal with structures with small random mistuning on each blade; this is thoroughly appropriate for situations in which the mistuning is due to manufacturing tolerances. Crack damage, on the other hand, typically occurs on a single blade and could have more severe local effects than the structural and material irregularities caused by manufacturing tolerances. As such, an analysis of this scenario is of great importance. If a newly created crack causes vibration localization, the excessive vibration amplitudes and local stresses could cause deterioration through high cycle fatigue and accelerate the crack propagation. In this paper, we study the effect of single crack on the vibratory response of a simplified aero-engine bladed-disk model which consists of cantilevered beams (blades) coupled with springs (inter-blade internal coupling). The individual blade of the bladed-disk is modeled as an Euler–Bernoulli beam. Although it is simplified, this model has been widely used in a variety of studies to qualitatively characterize the dynamic behavior of typical periodic and nearly periodic structures such as bladed-disks [6,7,11,12]. The assumed mode method is used to discretize the beam motion, which yields the system equation in the modal space. It should be noted that this modeling strategy is generic in nature, because for a real bladed-disk assembly we may also use the modal information of an uncoupled blade obtained via finite element analysis as assumed modes to reduce the corresponding system equation into the modal space. A fracture mechanics based model [13] is adopted to estimate the stiffness loss due to a crack on a single beam. By taking advantage of the unique property of periodic or nearly periodic structures, using the U-transformation approach [11] we then develop analytical and closed-form solutions to the free and forced vibrations of the bladed-disk with a single crack. A series of parametric analyses are performed. Specifically, we consider how the vibration localization level varies as a function of the various system parameters, such as inter-blade internal coupling, crack severity, excitation patterns, and number of blades.

2. Local crack effect modeling

A simplified bladed-disk model is illustrated in Fig. 1, which consists of N cantilevered beams coupled with massless linear springs. A crack on a blade/beam can cause local stiffness change, and correspondingly, result in changes in structural dynamic properties such as natural frequencies and mode shapes. In this section, we first evaluate how a crack changes the stiffness and natural frequencies of a single beam, by utilizing the methodology developed by Kim and Stubbs [13].

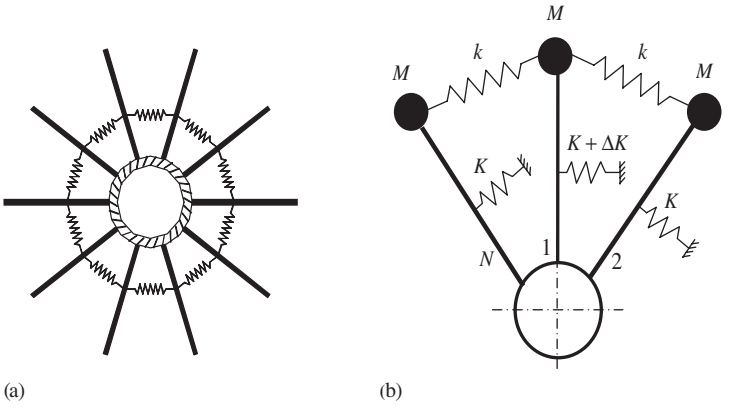

Fig. 1. (a) Bladed-disk model; (b) beam 1 with stiffness loss due to crack.

The Euler–Bernoulli theory is used to model the cantilevered beams. Consider a beam with a single crack. It is worth emphasizing that the main goal of this research is to explore qualitatively how various parameters in a cracked bladed-disk affect the vibration localization behavior. Therefore, for simplicity, here we assume that the crack extends over the entire width of the beam and use one parameter, the depth a to quantify the crack. The ith natural frequency and mode shape of the undamaged beam are ω_i and ϕ_i, respectively. When the crack appears, the ith natural frequency and mode shape become ω_i^* and ϕ_i^*, respectively. Neglecting the mass change and other geometrical changes due to the crack, we use a first-order perturbation method to quantify the changes in the natural frequencies due to the presence of the crack. The fractional changes in modal strain energy can be related to the fractional changes of the eigenvalues (frequencies) in the following manner [13,14]:

$$\frac{\delta\lambda_i}{\lambda_i} = \frac{\delta W_i}{W_i}, \tag{1}$$

where $W_i = \frac{1}{2}\int_0^L EI(\phi_i''(x))^2\,\mathrm{d}x$ and δW_i are the ith modal strain energy of the undamaged beam and its loss due to crack, respectively, and $\delta\lambda_i/\lambda_i$ is the fractional change of the ith eigenvalue due to crack. Here L is the beam length, E is the Young's modulus, and I is the area moment of inertia of the beam. The modal strain energy of the Euler–Bernoulli beam can be obtained in a straightforward manner. For an edge crack, the ith modal strain energy loss δW_i can be calculated from the energy release rate by implementing linear elastic fracture mechanics theory, which is expressed as [13–15]

$$\delta W_i = \left(\frac{\pi t(1-v^2)}{2E} a^2\sigma_k^2 G^2\right)_i, \tag{2}$$

where t is the beam width, v is the Poisson ratio, a is the crack depth at location x_k, $\sigma_k = \frac{1}{2}EH\phi_i''(x_k)$ represents the maximum flexural stress at location x_k along the longitudinal direction, and G is a geometrical factor depending on the ratio of crack depth a to beam height H [13,15],

$$G = 1.122 - 1.40(a/H) + 7.33(a/H)^2 - 13.08(a/H)^3 + 14.0(a/H)^4.$$

Substituting these expressions and Eq. (2) into Eq. (1) yields

$$\frac{\delta\lambda_i}{\lambda_i} = \frac{\delta W_i}{W_i} = \eta S_{ik}\left(\frac{a}{H}\right)_i^2,$$

where

$$S_{ik} = \left(\phi_i''(x_k)\right)^2 \Big/ \int_0^L \left(\phi_i''(x)\right)^2 \mathrm{d}x,$$

$$\eta = 0.25\pi t\left(1-v^2\right)G^2H^4/I.$$

Our interest is in the global dynamic properties of the bladed-disk. Therefore, the local beam modeling must enable us to characterize the global properties. For the nominal bladed-disk structure without any imperfection or crack, all the beams are identical. The springs, which are used to emulate the inter-blade internal coupling (Fig. 1), split the N-fold natural frequency of the structure consisting of uncoupled beams into a group of natural frequencies. While each beam has an infinite number of degrees-of-freedom (and the corresponding natural frequencies), we employ the assumed mode method to describe the beam motion, which is essentially a modal space approach. In order to gain fundamental insight into the response characteristics, here we only use the first beam mode $\phi_1(x)$ for discretization. This reduces each beam (blade) into a single degree-of-freedom structure. If one is interested in the effect of a crack on another frequency/mode group of the bladed-disk structure, one may use the corresponding beam mode for discretization. It should be noted that this modeling strategy is generic in nature, because for a practical finite element model of a bladed-disk assembly, we may also use the modal information of an uncoupled blade obtained via finite element analysis as assumed modes to reduce the corresponding system equation into the modal space. In the aforementioned simplified bladed-disk model, the undamaged (nominal) beam's natural frequency is denoted as $\omega_b(=\omega_1)$, and that of the damaged beam is denoted as $\omega_b^*(=\omega_1^*)$. Thus the fractional change in the natural frequency of the damaged beam can be obtained as

$$\frac{\omega_b^2-\omega_b^{*2}}{\omega_b^2} = \frac{-\Delta K}{K} = \eta S_{1k}\left(\frac{a}{H}\right)_1^2 \equiv -\Delta f, \tag{3}$$

where K is the equivalent nominal beam stiffness, and ΔK is the stiffness loss due to crack damage. In what follows we use Δf to represent the stiffness loss ratio. The stiffness loss can now be quantified, given parameters of the beam and the crack.

Table 1 lists 3 crack cases. The cross section and the length of the beam are, respectively, $0.032\,\mathrm{m}\times 0.016\,\mathrm{m}$ and $0.72\,\mathrm{m}$, and the material properties are $E=206\,\mathrm{GPa}$, $v=0.29$, and

Table 1
Damage scenarios and natural frequencies (rad/s) of cracked beam 1

Crack case	Location (x_k/L)	Depth (a/H)	ω_b	ω_b^*	Δf
1	0.5	0.160	325.1	321.9	−0.02
2	0.5	0.221	325.1	318.6	−0.04
3	0.5	0.287	325.1	311.8	−0.08

$\rho = 7650\,\mathrm{kg/m^3}$, which are the same as those used in Ref. [13]. These local results are later used in the study of global dynamic properties. It is interesting to note that while the crack depths are large, the corresponding frequency changes are very small. This implies that the frequency change information might not have sufficient sensitivity for crack damage detection.

3. Free vibration analysis and crack induced mode localization

We consider the free vibration of the simplified bladed-disk model shown in Fig. 1. For the damaged structure, we assume only one beam has a crack, which, for simplicity, is designated as blade 1. Cai et al. [11] developed a general theory to characterize the dynamic property of periodic structures with a single subsystem irregularity. In this section we use a similar approach to study specifically the effect of a reduced stiffness in one beam due to a crack. For such system, the free vibration is governed by the following equations:

$$\left(K + 2k - M\omega^2\right)q_i - k(q_{i+1} + q_{i-1}) = G_i \quad (i = 1, 2, \ldots, N), \tag{4}$$

where

$$G_i = \begin{cases} -\Delta K \cdot q_1 & (i = 1), \\ 0 & (i \neq 1). \end{cases}$$

Here q_i is the displacement of the ith beam, ω denotes the natural frequency of the bladed-disk structure, M and K are the equivalent mass and stiffness of each undamaged beam (i.e., $\omega_b = \sqrt{K/M}$), k is the coupling stiffness, and ΔK is the stiffness loss on the first beam. Note that, due to the cyclic symmetry, $q_0 \equiv q_N$ and $q_{N+1} \equiv q_1$. In this paper, we assume that the number of beams is even, e.g., $N = 20$.

By Eq. (4), it is obvious that the response of the ith beam q_i is coupled to the responses of its two nearest neighbors q_{i-1} and q_{i+1}. This equation can be greatly simplified by using the U-transformation. The U-transformation and the inverse U-transformation are defined as [11]

$$q_i = \frac{1}{\sqrt{N}} \sum_{r=1}^{N} \mathrm{e}^{\mathrm{j}(i-1)(r-1)\sigma} \cdot x_r \tag{5}$$

and

$$x_r = \frac{1}{\sqrt{N}} \sum_{i=1}^{N} \mathrm{e}^{-\mathrm{j}(i-1)(r-1)\sigma} \cdot q_i, \tag{6}$$

where $\sigma = 2\pi/N$ and $\mathrm{j} = \sqrt{-1}$. Substituting Eq. (5) into Eq. (4), we obtain

$$K\left\{1 - \lambda + 2R^2[1 - \cos(r-1)\sigma]\right\} \cdot x_r = -\Delta K \cdot q_1 \Big/ \sqrt{N} \quad (r = 1, 2, \ldots, N), \tag{7}$$

where $R^2 = k/K$ is the nondimensionalized coupling ratio (between the coupling stiffness and the uncoupled beam stiffness), and $\lambda = \omega^2/\omega_b^2$ is the eigenvalue of the bladed-disk structure. It is worth mentioning that after the U-transformation, in Eq. (7) the displacement components are almost decoupled. Substituting Eq. (7) into Eq. (5), we recover the modal amplitude of the

ith beam,

$$q_i = \frac{-\Delta f \cdot q_1}{N} \sum_{r=1}^{N} \frac{\cos[(i-1)(r-1)\sigma]}{1-\lambda+2R^2[1-\cos(r-1)\sigma]} \quad (i=1,2,\ldots,N). \tag{8}$$

For the undamaged system, $\Delta K = 0$, and Eq. (7) yields

$$1-\lambda+2R^2[1-\cos(r-1)\sigma]=0 \quad (r=1,2,\ldots,N), \tag{9}$$

which gives the eigenvalues of the undamaged structure (denoted as λ_{0r}),

$$\lambda_{0r} = 1+2R^2[1-\cos(r-1)\sigma] \quad (r=1,2,\ldots,N). \tag{10}$$

Note the corresponding undamaged natural frequencies are $\omega_{0r} = \sqrt{\lambda_{0r}}\omega_b$. It is easy to find out that $\omega_{0r} = \omega_{0,N-r+2}$, and the number of distinct natural frequencies is $N/2+1$. The lower and upper bounds of the frequency group ω_{0r} are, respectively,

$$\omega_L = \omega_b, \quad \omega_U = \sqrt{1+4R^2}\omega_b. \tag{11}$$

The frequency band within these two bounds is called the pass-band, and it is well known that if a frequency falls out of the pass-band, the corresponding vibratory response will be localized [16].

We use the undamaged eigenvalue λ_{0r} to further simplify the notations used in the analysis. When $q_1 \neq 0$, from Eq. (8) we can get

$$-\Delta f = N \Big/ \sum_{r=1}^{N} \frac{1}{\lambda_{0r}-\lambda}. \tag{12}$$

Given a stiffness loss ratio, from the above equation we can solve for $N/2+1$ eigenvalues (and thus natural frequencies) of the damaged structure, whose corresponding modes all have $q_1 \neq 0$. This can be illustrated by using a graphical representation developed by Cai et al. [11]. As shown

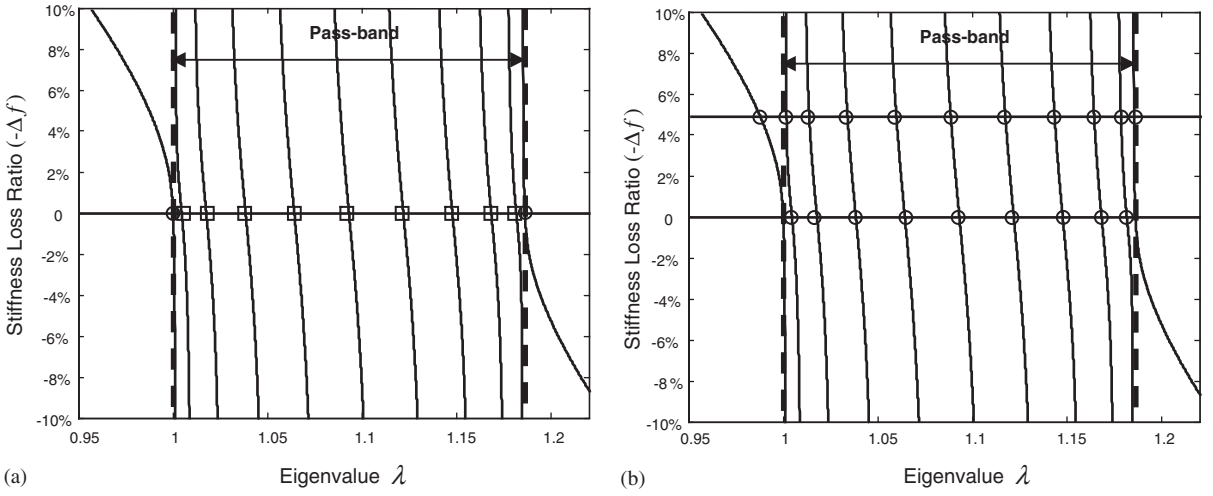

Fig. 2. Natural frequencies of undamaged (a) and damaged bladed-disk (b): ○ distinct frequency; □ two-fold frequency. The first frequency of the damaged bladed-disk falls out of the pass-band immediately, and the corresponding mode becomes localized.

in Fig. 2, these $N/2+1$ eigenvalues are given as the intersection points between a family of frequency curves (see Eq. (12)) and the horizontal line corresponding to the stiffness loss ratio. Here the vertical coordinates represent the stiffness loss ratio, and the horizontal coordinates of the intersection points are the eigenvalues λ of the damaged structure. In general, $N/2+1$ different eigenvalues λ_{0r} lead to $N/2+1$ curves corresponding to the right-hand side of Eq. (12). For our specific bladed-disk structure example with 20 beams, we can obtain 11 distinct natural frequencies from Eq. (12). It is worth emphasizing that, with the stiffness loss $\Delta K<0$ (i.e., $-\Delta f>0$) caused by a single crack, none of the eigenvalues λ of the damaged bladed-disk can be greater than $1+4R^2$; otherwise, Eq. (12) cannot hold because the right-hand side would be negative.

The above $N/2+1$ eigenvalues λ are solved under the condition $q_1 \neq 0$, so the rest $N/2-1$ eigenvalues λ must correspond to modes whose first component is given as $q_1 = 0$, which can be obtained directly from Eq. (7). Indeed, under the condition that $q_1 = 0$, these eigenvalues λ are not affected by the crack damage at all and are equal to λ_{0r} ($r = 2, 3, \ldots, N/2$). As shown in Fig. 2, these eigenvalues are given as the 9 (i.e., $N/2-1$) intersection points between the frequency curves and the original horizontal axis (i.e., $-\Delta f = 0$). From Eqs. (4) and (10), the corresponding modes can be easily solved as

$$\begin{aligned} q_1 &= 0 \\ q_3/q_2 &= 2\cos(r-1)\sigma \qquad (r = 2, 3, \ldots, N/2), \\ q_i &= -q_{i-2} + 2q_{i-1}\cdot\cos(r-1)\sigma \qquad (i = 4, 5, \ldots, N). \end{aligned} \tag{13}$$

These modes are obviously extended modes without localization.

Our special interest here is focused on whether vibration mode localization could occur when crack damage occurs. Since all the eigenvalues of the damaged bladed-disk must be smaller than $1+4R^2$ (which corresponds to the upper bound of the pass-band), mode localization can only occur when any of the corresponding eigenvalues are smaller than 1 (which corresponds to the lower bound of the pass-band). In what follows we find approximately the analytical solution to the eigenvalues smaller than 1. Setting $N \to \infty$ yields the following relation [11]:

$$\lim_{n\to\infty} \frac{1}{N} \sum_{r=1}^{N} \frac{\cos[(i-1)(r-1)\sigma]}{1-\lambda+2R^2[1-\cos(r-1)\sigma]} = \frac{1}{\pi}\int_0^{\pi} \frac{\cos(i-1)\theta\,\mathrm{d}\theta}{1-\lambda+2R^2(1-\cos\,\theta)}.$$

Eq. (8) can then be rewritten as, under the condition that N is large,

$$\frac{q_i}{q_1} = \frac{q_{N-i+2}}{q_1} \approx -\Delta f \frac{1}{2R^2\pi}\int_0^{\pi} \frac{\cos(i-1)\theta\,\mathrm{d}\theta}{\varepsilon-\cos\,\theta}, \tag{14}$$

where we define $\varepsilon = (1-\lambda+2R^2)/2R^2$ (recall here we have $\lambda<1$, i.e., $\varepsilon>1$). After some derivations, we can obtain

$$\frac{q_i}{q_1} = \frac{q_{N-i+2}}{q_1} \approx \frac{-\Delta f \cdot \left(\varepsilon - \sqrt{\varepsilon^2-1}\right)^{i-1}}{2R^2\sqrt{\varepsilon^2-1}}. \tag{15}$$

When $i = 1$, the above equation leads to

$$\frac{-\Delta f}{2R^2\sqrt{\varepsilon^2 - 1}} \approx 1,$$

which yields one and only one solution $\lambda_1(<1)$ (i.e., the first eigenvalue of the damaged bladed-disk),

$$\lambda_1 \approx 1 + 2R^2 - 2R^2\sqrt{1 + \left(\Delta f/2R^2\right)^2}. \tag{16}$$

Clearly, with the crack damage, the eigenvalue of the first mode immediately falls out of the pass-band, which means the first mode immediately becomes localized. On the other hand, with a single crack damage, only the first mode is localized. Table 2 lists the first eigenvalue λ_1 of the damaged bladed-disk with different number of blades. The approximate solution given by Eq. (16) (which is derived under the assumption $N \to \infty$) has close agreement with the actual λ_1 obtained by numerically solving the eigenvalue problem.

Recall that, for the undamaged structure, the first eigenvalue is $\lambda_{01} = 1$ (see Eq. (10)). When the stiffness loss is small and $(\Delta f/2R^2)^2 \ll 1$, the difference between the first eigenvalue of the damaged structure and that of the undamaged structure is approximately equal to $(\Delta f/2R)^2$, which is small. Nevertheless, the first vibration mode of the damaged structure is localized and thus is significantly different from that of the undamaged structure. In order to characterize this localized first vibration mode which has $q_1 \neq 0$, we define the attenuation rate γ of this mode as

$$\gamma = \frac{q_2}{q_1}. \tag{17}$$

Taking the logarithm of Eq. (15) and using Eq. (16), we can easily show that

$$\log q_{i+1} - \log q_i = \log q_{N-i+1} - \log q_{N-i+2} = \log \gamma \quad \left(i = 1, 2, \ldots, N/2\right) \tag{18}$$

and

$$\gamma = \sqrt{1 + \left(\Delta f/2R^2\right)^2} - \left|\Delta f/2R^2\right|. \tag{19}$$

At this point, we can conclude that for the localized first vibration mode, the cracked beam has the highest amplitude (as γ must be smaller than 1), whereas the other beams have exponentially decaying amplitudes. Meanwhile, the attenuation rate γ, which is an indicator of the degree of vibration localization, depends only on the ratio of stiffness loss ratio to coupling, $\Delta f/R^2$. It should be emphasized that for the original undamaged bladed-disk, in the first mode all the beams must have the same vibration amplitude. This can also be demonstrated by letting the crack

Table 2
Eigenvalue λ_1 of bladed-disk with $R = 0.2$, $\Delta f = -0.08$

Number of blades	Actual λ_1	Approximate λ_1
6	0.9663	0.9669
10	0.9668	0.9669
20	0.9669	0.9669

induced stiffness loss go to zero in Eq. (19). In that case ($\Delta f = 0$), the attenuation rate becomes 1 which means no decay in vibration amplitude. It should be noted that if $(\Delta f/2R^2)^2 \ll 1$, the attenuation rate γ is approximately equal to $1 - |\Delta f/2R^2|$, that is, γ is additively inverse to $|\Delta f/R^2|$. Therefore, it is clear that the degree of localization increases with more severe cracks or smaller coupling ratios, the latter being consistent with all previous studies on randomly mistuned systems.

Figs. 3a and b illustrate the localized first vibration mode where the beams away from the cracked beam (i.e. beam 1) have exponentially decaying amplitudes. The exponential decay rate is

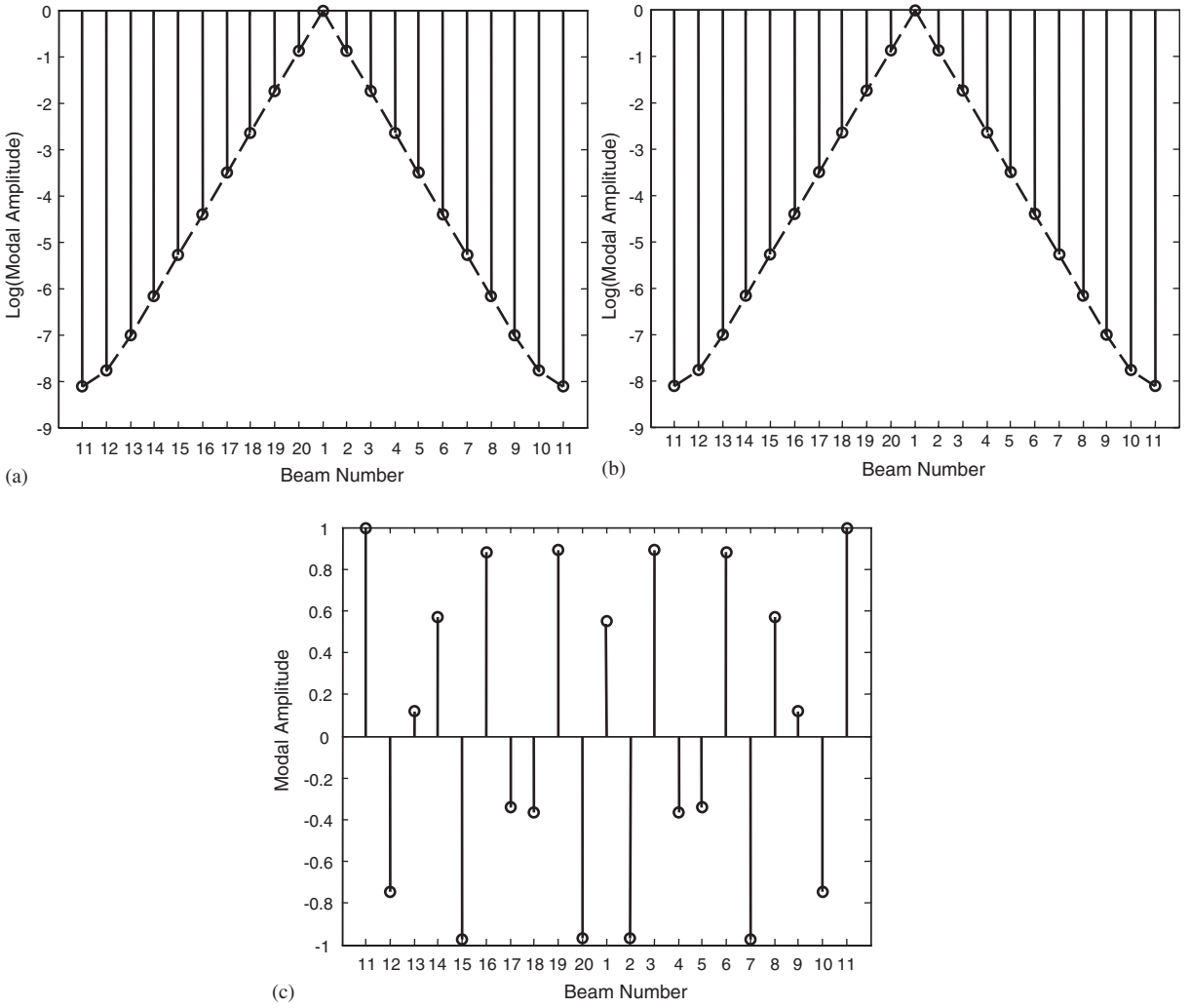

Fig. 3. Localized and non-localized modes of damaged structure with $N = 20$: (a) 1st mode and slope of the envelope $\log\gamma = -0.88$ when $R = 0.2$ and $\Delta f = -0.08$; (b) 1st mode and slope of the envelope $\log\gamma = -0.88$ when $R = 0.1$ and $\Delta f = -0.02$; (c) 16th mode when $R = 0.2$ and $\Delta f = -0.08$. (Note: in panel c the modal amplitude is not plotted in logarithm scale, because this 16th mode is not localized and some modal components have negative signs.)

consistent with the analytical solution $\log\gamma$ (see Eq. (18)). Figs. 3a and b also show that, for damaged bladed-disks with the same ratio of stiffness loss to coupling, the degrees of localization are the same. Fig. 3c shows the 16th mode of the damaged structure, which is clearly not localized. The results given in Fig. 3 are obtained by numerical solution, and are in complete agreement with the aforementioned analytical study.

4. Forced vibration analysis

4.1. General solution of the response under excitations with spatially harmonic distribution

In this section we discuss the forced vibration response of a damaged bladed-disk structure. The external force studied in this research has a spatially harmonic distribution which is the usual case for aero-engine applications, i.e., the force acting on the ith beam is $F\mathrm{e}^{\mathrm{j}\omega_e t+\phi_i}$, where $\mathrm{j}=\sqrt{-1}$, ω_e is the excitation frequency, and $\phi_i = 2\pi C(i-1)/N$. Here $C(C=0,1,2,\ldots,N)$ is an integer which is often referred to as the engine order. Using Eq. (1) as basis, we can easily obtain the equations for the forced response,

$$\left(1+2R^2-\Omega^2+\mathrm{j}\cdot 2\xi\Omega\right)q_i - R^2\left(q_{i+1}+q_{i-1}\right) = F_i/\omega_b^2 - \Delta f\cdot q_1 \quad (i=1), \tag{20a}$$

$$\left(1+2R^2-\Omega^2+\mathrm{j}\cdot 2\xi\Omega\right)q_i - R^2\left(q_{i+1}+q_{i-1}\right) = F_i/\omega_b^2 \quad (i=2,3,\ldots,N), \tag{20b}$$

where ξ is the damping ratio, $\Omega=\omega_e/\omega_b$ is the nondimensionalized excitation frequency, and $F_i=(F/M)\mathrm{e}^{\mathrm{j}\phi_i}$. Using the U-transformation and the inverse U-transformation defined in Eqs. (5) and (6), we can decouple the above N equations and obtain

$$\left[1+2R^2-\Omega^2+\mathrm{j}\cdot 2\xi\Omega-2R^2\cos((r-1)\cdot\sigma)\right]\cdot x_r = \frac{1}{\sqrt{N}}\left[\frac{F}{M\omega_b^2}\sum_{p=1}^{N}\mathrm{e}^{-\mathrm{j}(r-C-1)(p-1)\sigma}-\Delta f\cdot q_1\right],$$

which, in turn, yields the response amplitude of the ith beam,

$$q_i = \frac{1}{N}\sum_{r=1}^{N}\mathrm{e}^{\mathrm{j}(i-1)(r-1)\sigma}\cdot\frac{\left(F/M\omega_b^2\right)\sum_{p=1}^{N}\mathrm{e}^{-\mathrm{j}(r-C-1)(p-1)\sigma}-\Delta f\cdot q_1}{1-\Omega^2+2R^2[1-\cos(r-1)\sigma]+\mathrm{j}\cdot 2\xi\Omega}. \tag{21}$$

Setting $i=1$, we can get the response of the first beam as

$$q_1 = \frac{F}{M\omega_b^2}\frac{\dfrac{1}{1-\Omega^2+2R^2(1-\cos\ C\sigma)+\mathrm{j}\cdot 2\xi\Omega}}{1+\dfrac{\Delta f}{N}\displaystyle\sum_{r=1}^{N}\frac{1}{1-\Omega^2+2R^2[1-\cos(r-1)\sigma]+\mathrm{j}\cdot 2\xi\Omega}}. \tag{22a}$$

Since $M\omega_b^2 = K$, Eq. (22a) can be rewritten as

$$q_1 = \frac{F}{K} \frac{\dfrac{1}{1-\Omega^2+2R^2(1-\cos C\sigma)+\mathrm{j}\cdot 2\xi\Omega}}{1+\dfrac{\Delta f}{N}\displaystyle\sum_{r=1}^{N}\dfrac{1}{1-\Omega^2+2R^2[1-\cos(r-1)\sigma]+\mathrm{j}\cdot 2\xi\Omega}}. \tag{22b}$$

Substituting Eq. (22a) into Eq. (21), we have the forced responses of other beams,

$$q_i = q_1 \cdot \left\{ 1+\frac{\Delta f}{N}\sum_{r=1}^{N}\frac{1}{1-\Omega^2+2R^2[1-\cos(r-1)\sigma]+\mathrm{j}\cdot 2\xi\Omega} - \frac{\Delta f}{N}\sum_{r=1}^{N}\frac{\cos(i-1)(r-1)\sigma}{1-\Omega^2+2R^2[1-\cos(r-1)\sigma]+\mathrm{j}\cdot 2\xi\Omega}\right\}, \quad i=2,3,\ldots,N. \tag{23}$$

Eqs. (22) and (23) coonstitute the general solution of bladed-disk response under the spatially harmonic excitation.

4.2. Response of undamaged bladed-disk

For the undamaged bladed-disk, the forced response behaviors have been extensively studied [6]. Such response, denoted as $q_0(\Omega)$ hereafter, can now be easily obtained from Eqs. (22b) and (23) with $\Delta f = 0$,

$$q_0(\Omega) = \frac{F}{K}\frac{1}{1-\Omega^2+2R^2(1-\cos\ C\sigma)+\mathrm{j}\cdot 2\xi\Omega}. \tag{24}$$

Clearly, at a given excitation frequency, all the beams experience the same amplitude $\tilde{q}_0(\Omega)$,

$$\tilde{q}_0(\Omega) = \frac{F}{K}\frac{1}{\sqrt{\left(\lambda_{C+1}-\Omega^2\right)^2+(2\xi\Omega)^2}}, \tag{25}$$

where $\lambda_{C+1} = 1+2R^2[1-\cos(C\cdot\sigma)]$, which is the $(C+1)$th eigenvalue of the undamaged structure. The nondimensionalized resonant frequency is

$$\Omega_{0r} = \sqrt{\lambda_{C+1}-2\xi^2} \tag{26}$$

and the corresponding resonant amplitude is

$$\tilde{q}_{0\mathrm{res}} = \frac{F}{K}\frac{1}{2\xi\sqrt{\lambda_{C+1}-\xi^2}}. \tag{27}$$

While these results are the same obtained by Wei and Pierre [6], in what follows these are used as a baseline for comparing with the response of the damaged bladed-disk. Eq. (27) shows that, under the same force amplitude, as C increases from 0 to $N/2$, the resonant amplitude $\tilde{q}_{0\mathrm{res}}$ decreases to reach its minimum, whereas as C increases from $N/2$ to N, $\tilde{q}_{0\mathrm{res}}$ increases to reach its maximum.

When C is equal to 0 or N, if $\xi \ll 1$, the resonance occurs approximately at the non-dimensionalized frequency 1 and $\tilde{q}_{0\text{res}} \approx (F/K)(1/2\xi)$. Eq. (27) also indicates that $\tilde{q}_{0\text{res}}$ increases as the coupling R^2 decreases when C is unequal to 0 or N.

4.3. Response under crack damage

Here we study the forced response behavior of the damaged structure with crack. Comparing Eq. (22b) with Eq. (24), one can see that the damage effect on the first beam appears in the denominator of Eq. (22b), which is now defined as

$$g(\Omega) = 1 + \frac{\Delta f}{2R^2}\frac{1}{N}\sum_{r=1}^{N}\frac{1}{\eta - \cos(r-1)\sigma}, \tag{28a}$$

where

$$\eta = \frac{1 - \Omega^2 + 2R^2 + \mathrm{j}2\xi\Omega}{2R^2}. \tag{28b}$$

Based upon Eq. (22b), the forced response of the first beam can then be expressed as

$$q_1(\Omega) = q_0(\Omega)/g(\Omega). \tag{29}$$

Recall that $q_0(\Omega)$ is the undamaged response (of all beams). Clearly, $g(\Omega)$ characterizes the amplification effect due to crack damage.

As discussed in Section 3, the first natural frequency of the damaged bladed-disk structure λ_1 is smaller than 1 (which corresponds to the lower bound of the pass-band) and thus corresponds to the localized vibration mode. Therefore, here we specifically study the forced response of the damaged bladed-disk when the nondimensionalized excitation frequency Ω is smaller than 1. By letting $N \to \infty$, the limit of the series summation in Eq. (28a) becomes a definite integral, and if $\Omega < 1$ and $\xi/R^2 \approx 0$, (i.e. under small damping assumption $\xi \ll 1$, $\mathrm{Re}(\eta) > 1$, and $\mathrm{Im}(\eta) \approx 0$), it yields

$$\lim_{n\to\infty}\frac{1}{N}\sum_{r=1}^{N}\frac{1}{\eta - \cos(r-1)\sigma} = \frac{1}{\sqrt{\eta^2 - 1}}.$$

Eq. (28a) can then be written as, approximately,

$$g(\Omega) \approx 1 + \frac{\Delta f}{2R^2}\frac{1}{\sqrt{\eta^2 - 1}}, \tag{30}$$

or

$$g(\Omega) \approx 1 - 1/\left\{\left[\Omega^4 - 2\Omega^2\left(1 + 2R^2 + 2\xi^2\right) + \left(1 + 4R^2\right)\right]/\Delta f^2 + j4\xi\Omega\left(1 + 2R^2 - \Omega^2\right)/\Delta f^2\right\}^{1/2}.$$

After some derivations, it can be shown that if $\xi\Omega(1 + 2R^2 - \Omega^2)/\Delta f^2 \approx 0$, which is often satisfied when damping is small, the minimum of $|g(\Omega)|$ and, hence the maximum amplification, can be reached when the following condition is satisfied,

$$\left[\Omega^4 - 2\Omega^2\left(1 + 2R^2 + 2\xi^2\right) + \left(1 + 4R^2\right)\right]/\Delta f^2 = 1. \tag{31}$$

The above equation gives the resonant frequency that is smaller than 1,

$$\Omega_r^2 = \left(1 + 2R^2 + 2\xi^2\right) - \sqrt{4R^4 + 4\xi^2\left(1 + 2R^2 + \xi^2\right) + \Delta f^2}. \tag{32}$$

Note that for the purpose of simplification in discussion, here we tacitly assume that when $|g(\Omega)|$ reaches minimum, the response exhibits resonance. The following studies will indicate that this simplification is a very close approximation to the actual resonance result. Under the small damping assumption $\xi \ll 1$, the nondimensionalized resonant frequency given in Eq. (32) can be further simplified as

$$\Omega_r^2 \approx 1 + 2R^2 - 2R^2\sqrt{1 + \left(\Delta f/2R^2\right)^2}, \tag{33}$$

which is the same as the eigenvalue λ_1 corresponding to the localized first mode discussed in Section 3 of the paper. It is worth emphasizing that this resonance frequency is independent of the engine order C. In other words, regardless of the specific engine order, the bladed-disk with crack damage will experience (localized) resonance at the frequency given by Eq. (33).

Next consider the corresponding resonant peak value. Substituting Eq. (31) into Eq. (30) yields

$$g(\Omega_r) = 1 - \left[1 + \mathrm{j}4\xi\Omega_r\left(1 + 2R^2 - \Omega_r^2\right)/\Delta f^2\right]^{-1/2}. \tag{34}$$

Using a Taylor series expansion, we obtain

$$g(\Omega_r) \approx \mathrm{j}2\xi\Omega_r\left(1 + 2R^2 - \Omega_r^2\right)/\Delta f^2. \tag{35}$$

Hence, the resonant amplitude of beam 1 at the nondimensionalized resonant frequency Ω_r is given as

$$\tilde{q}_{1\mathrm{res}} = \frac{F}{K}\frac{\Delta f^2}{2\xi\Omega_r\left(1 + 2R^2 - \Omega_r^2\right)\sqrt{\left(\lambda_{C+1} - \Omega_r^2\right)^2 + (2\xi\Omega_r)^2}}, \tag{36a}$$

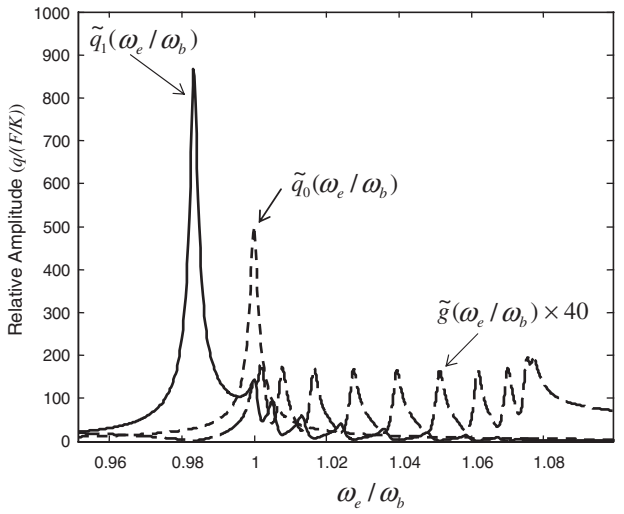

Fig. 4. $\tilde{q}_1(\omega_e/\omega_b)$, $\tilde{q}_0(\omega_e/\omega_b)$ and $\tilde{g}(\omega_e/\omega_b)$ with $N = 20$, $R = 0.2$, $\Delta f = -0.08$, $\xi = 0.001$, and $C = 0$.

or,

$$\tilde{q}_{1\mathrm{res}} = \frac{F}{K} \frac{\left(\Delta f/2R^2\right)^2}{2\xi\Omega_r\sqrt{1+\left(\Delta f/2R^2\right)^2}\sqrt{\left[\sqrt{1+\left(\Delta f/2R^2\right)^2}-\cos C\sigma\right]^2+\left(\xi\Omega_r/R^2\right)^2}}. \tag{36b}$$

The above analysis gives a qualitative measure of the forced response of beam 1 at resonant frequency Ω_r. The approximate solutions to the resonant frequency Ω_r and the associated peak response are given in Eqs. (33) and (36), respectively. For verification purpose, in Fig. 4 we plot $\tilde{q}_1$, $\tilde{q}_0$, and $\tilde{g}$ under engine order $C=0$ solved numerically by direct solution of the forced vibration problem. Clearly, the minima of $\tilde{g}$ result in resonant peaks in response $\tilde{q}_1$. The first minimum of $\tilde{g}$ leads to the most significant resonant response of blade 1. This frequency is indeed the one obtained in Eq. (33). The other minima of $\tilde{g}$ are much larger than the first minimum. In addition, $\tilde{q}_0$ decreases drastically when the excitation frequency is away from the undamaged structure's resonant frequency Ω_{0r}. Consequently, the other resonant peaks (that the cracked blade experiences) are much lower than the first one. The approximate solution of the most significant resonant peak given by Eq. (36a) has very good agreement with the actual result over a wide range of damping values, as demonstrated in Fig. 5.

We now compare the vibratory responses of all the beams, and study the vibration amplitude localization. When $\Omega<1$ (i.e., $\mathrm{Re}(\eta)>1$), for large N, Eq. (23) can be rewritten as

$$q_i = q_{N-i+2} \approx q_1 \cdot \left\{1+\frac{\Delta f}{2R^2}\frac{1-\left(\eta-\sqrt{\eta^2-1}\right)^{i-1}}{\sqrt{\eta^2-1}}\right\} \quad (i=2,3,\ldots,N/2+1). \tag{37}$$

Under the small damping assumption $\xi \ll 1$, we have $\mathrm{Im}(\eta)\approx 0$. In virtue of Eq. (28b), we have,

$$0<\eta-\sqrt{\eta^2-1}<1,$$

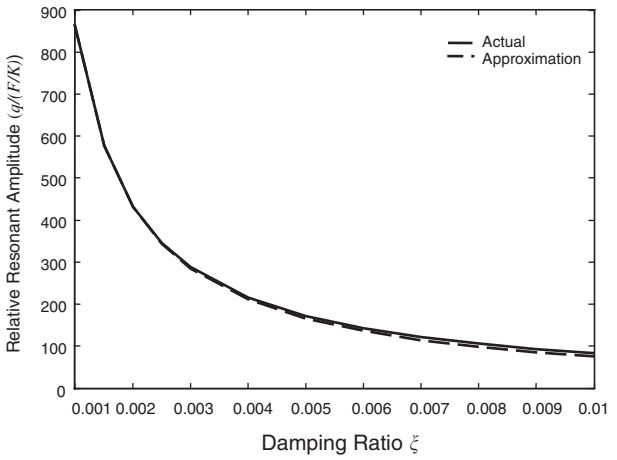

Fig. 5. Resonant amplitude of beam 1 at Ω_r for the damaged structure versus damping ratio with $N=20$, $R=0.2$, $\Delta f=-0.08$, and $C=0$.

or

$$0<1-\left(\eta-\sqrt{\eta^2-1}\right)^{i-1}<1 \quad (i=2,3,\ldots,N/2+1).$$

Recalling that $\Delta f/2R^2<0$, based upon Eq. (37) we conclude

$$q_1\cdot\left\{1+\frac{\Delta f}{2R^2}\frac{1}{\sqrt{\eta^2-1}}\right\}<q_i=q_{N-i+2}<q_1 \quad (i=2,3,\ldots,N/2+1),$$

or

$$q_0<q_i=q_{N-i+2}<q_1 \quad (i=2,3,\ldots,N/2+1). \tag{38}$$

Clearly, when the nondimensionalized excitation frequency $\Omega<1$, the damaged beam has the largest amplitude among all the beams, and the amplitude of any beam of the damaged system is also larger than that of the corresponding undamaged system under the same excitation frequency. This clearly illustrates the effect of forced vibration localization.

Particularly, when $\Omega=\Omega_r$, the amplitude of the damaged beam reaches its resonant peak value. We then analyze the vibration amplitude of all the beams at this frequency. Substituting Eq. (33) into Eq. (37) yields

$$q_i(\Omega_r)/q_{1\mathrm{res}}=q_{N-i+2}(\Omega_r)/q_{1\mathrm{res}}\approx\left[\sqrt{1+\left(\Delta f/2R^2\right)^2}-\left|\Delta f/2R^2\right|\right]^{i-1}<1 \quad (i=2,3,\ldots,N/2+1). \tag{39}$$

It is important to note that (1) the forced vibration amplitude decays uniformly between adjacent beams; and (2) the decay rate is the same as that given in Eq. (19) under free vibration analysis. Also, the decay rate is independent of the engine order C. For a weakly coupled bladed-disk, (i.e., $|\Delta f/R^2|\gg 1$), $\sqrt{1+(\Delta f/2R^2)^2}+\Delta f/2R^2\ll 1$, and thus $q_i(\Omega_r)/q_{1\mathrm{res}}=q_{N-i+2}(\Omega_r)/q_{1\mathrm{res}}\ll 1$. Clearly, the forced response at the resonant frequency Ω_r is extremely localized, with the damaged beam having the largest amplitude. The decay rate, $\sqrt{1+(\Delta f/2R^2)^2}-|\Delta f/2R^2|$, monotonically decreases with respect to $|\Delta f/2R^2|$, which is consistent with the conclusion under free vibration analysis.

In what follows we discuss the effects of various parameters.

4.3.1. Effect of coupling

For a very weakly coupled bladed-disk (i.e., $|\Delta f/R^2|\gg 1$), one can easily see that Ω_r is approximately equal to $\sqrt{1-|\Delta f|}$ (see Eq. (33)). Substituting this into Eq. (36a) and neglecting the damping, we find $\tilde{q}_{1\mathrm{res}}\approx(F/K)[1/(2\xi\sqrt{1-|\Delta f|})]$, when $C=0$ or N. Compared with that of undamaged bladed-disk (see the discussion under Eq. (27)), the resonant response amplitude of the damaged beam 1 at the resonant frequency Ω_r is amplified by a factor of $1/\sqrt{1-|\Delta f|}$.

Now consider the cracked beam amplitude for a moderately coupled bladed-disk (i.e., $|\Delta f/R^2|\approx 1$). As the coupling ratio increases, the resonant frequency Ω_r and $(1+2R^2-\Omega_r^2)$

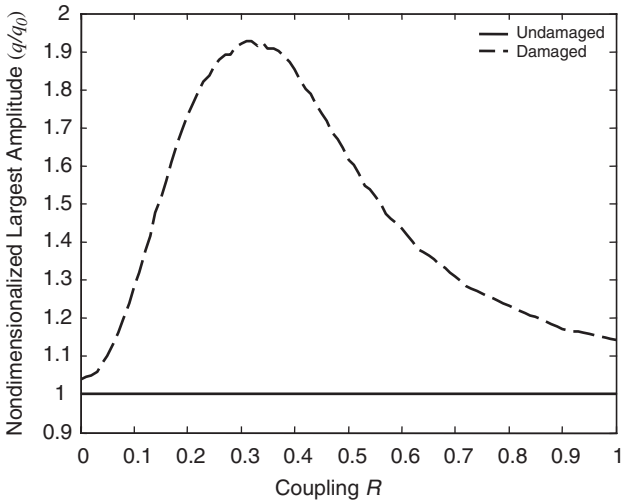

Fig. 6. Resonant amplitude of beam 1 at Ω_r for the undamaged and damaged structures versus coupling with $N = 20$, $\xi = 0.001$, $\Delta f = -0.08$, and $C = 0$.

(in Eq. (36a)) increase gradually, but $\sqrt{(\lambda_{C+1} - \Omega_r^2)^2 + (2\xi\Omega_r)^2}$ (in Eq. (36a)) decreases rapidly, resulting in a fast increase of the resonant response amplitude $\tilde{q}_{1\text{res}}$.

For a strongly coupled bladed-disk (i.e., $|\Delta f/R^2| \approx 1$), the resonant frequency Ω_r approaches 1 and $(1 + 2R^2 - \Omega_r^2)$ increases drastically as the coupling increases, while $\sqrt{(\lambda_{C+1} - \Omega_r^2)^2 + (2\xi\Omega_r)^2}$ decreases slowly. This causes the resonant response amplitude $\tilde{q}_{1\text{res}}$ to decrease. These results are summarized in Fig. 6, which shows the resonant response of beam 1 at Ω_r as a function of the structural coupling for the undamaged and damaged cases under engine order $C = 0$. When $C = 0$, although the structural coupling changes, the resonant response amplitude of the undamaged bladed-disk remains constant. For the particular case shown, the stiffness loss is $\Delta f = -0.08$. For a very weak coupling ($R = 0.02$), the resonant response amplitude of the damaged beam 1 at Ω_r is slightly larger than that of the undamaged bladed-disk; this amplification factor is due to the crack damage and is 1.04, which is approximately equal to $1/\sqrt{1 - |\Delta f|}$. For a moderately coupled bladed-disk with $|\Delta f/R^2| \approx 1$, $\sqrt{(\lambda_{C+1} - \Omega_r^2)^2 + (2\xi\Omega_r)^2}$ is inversely proportional to R^2. This is confirmed in Fig. 6 by the rapid increase in the resonant amplitude of beam 1, where the coupling increases from small to moderate levels. On the other hand, for a strongly coupled bladed-disk, the resonant amplitude of beam 1 decreases as the coupling increases, as shown in Fig. 6. Fig. 6 also shows that the transition between these two behaviors happens at $R \approx 0.3$.

Fig. 7 shows the forced responses of the undamaged and damaged bladed-disks. Here the largest beam amplitude throughout the bladed-disk structure is plotted against the external excitation frequency. In Fig. 7a it is shown that, for a very weak coupling ($R = 0.02$), the resonant amplitude at Ω_r is larger than that of the second peak. The second peak of the damaged bladed-disk almost coincides with the peak of the original undamaged structure. The reason for this is

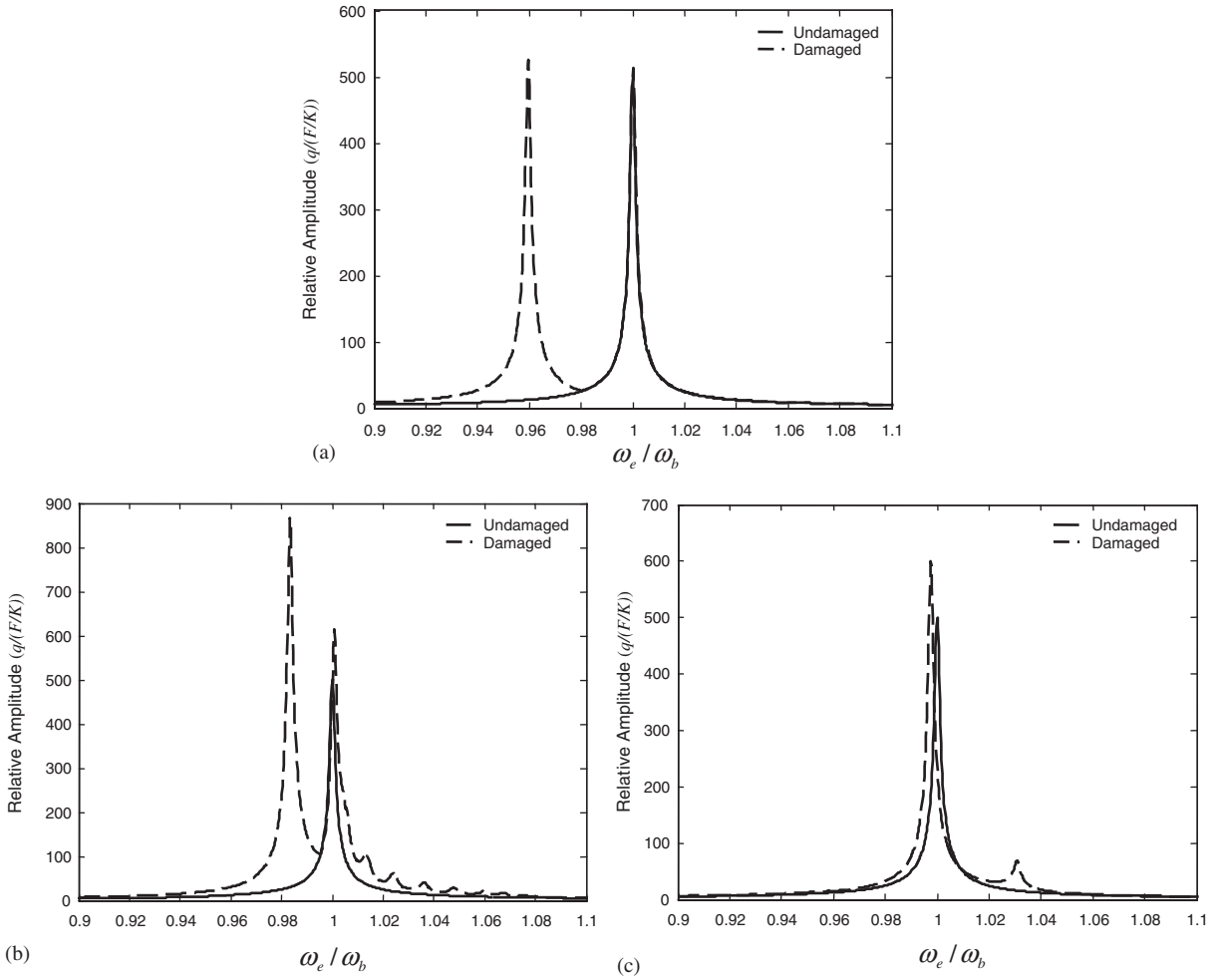

Fig. 7. Largest beam amplitudes of undamaged and damaged structures versus excitation frequency with $N = 20$, $\xi = 0.001$, $\Delta f = -0.08$, and $C = 0$ for various coupling: (a) $R = 0.02$; (b) $R = 0.2$; (c) $R = 0.85$.

obvious: the crack damage reduces the stiffness of only one beam thus the cracked beam experiences peak response at a new (smaller) resonant frequency Ω_r (with vibration localization), whereas other beams are almost not affected under very weak coupling. Recall that the original undamaged bladed-disk has only one resonant peak under any engine order C. Therefore, except for the additional peak, the forced response of the damaged bladed-disk at other frequencies is almost the same as that of the undamaged bladed-disk. Fig. 7b illustrates the system behavior under moderate coupling ($R = 0.2$). Similarly, an additional peak appears, which corresponds to the cracked beam's resonance. Due to the increased coupling, crack damage affects the dynamic behavior of other beams more significantly. Therefore, other resonant peaks also appear, but with smaller amplitudes. It is worth noting that, although the amplitudes of the first two peaks are both larger than $\tilde{q}_{0\text{res}}$ (the resonant amplitude of the undamaged bladed-disk), the first peak is much higher. Compared with the two peaks shown in Fig. 7a, the two main peaks in Fig. 7b shift to

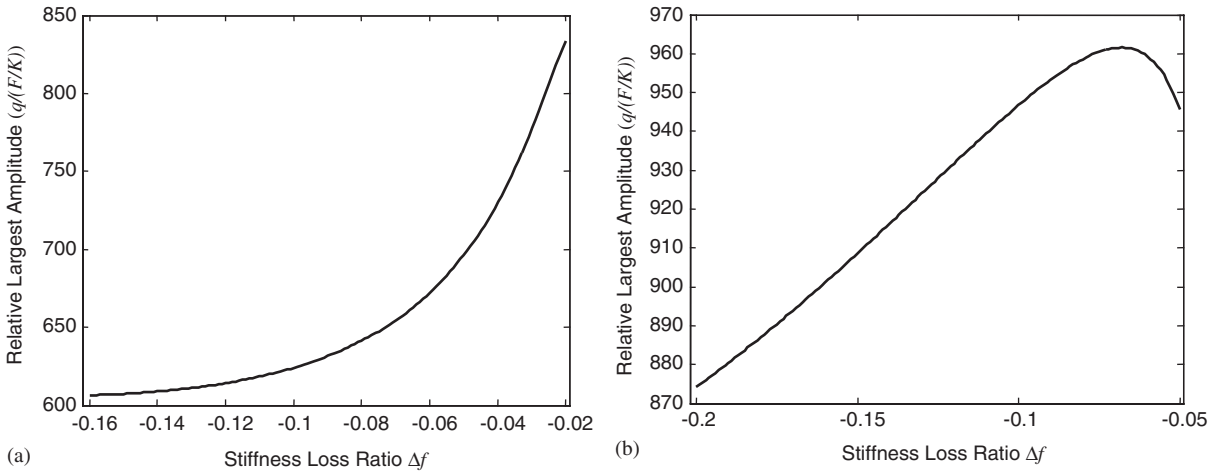

Fig. 8. Resonant amplitude of beam 1 at Ω_r for the damaged structure versus stiffness loss ratio Δf with $N = 20$, $\xi = 0.001$, and $C = 0$ for different coupling R: (a) $R = 0.1$; (b) $R = 0.3$.

higher frequencies, as the coupling increases. Fig. 7c shows that, for a strongly coupled system ($R = 0.85$), the first peak of the damaged response almost coincides with the peak of the undamaged bladed-disk's response. This is because, for a strongly coupled structure (i.e. $|\Delta f/R^2| \ll 1$), Ω_r obtained from Eq. (33) approaches 1. Compared with that of the first peak shown in Fig. 7b, the amplitude of the first peak shown in Fig. 7c decreases significantly.

4.3.2. Effect of crack severity

Intuitively, the vibratory behavior of the damaged bladed-disk is dependent on the crack severity (indicated by Δf), as shown in Eq. (36a). From Eq. (36b), we can further see that the forced response is actually dependant upon the ratio $|\Delta f/R^2|$. Clearly, a decrease in the stiffness loss due to a crack and an increase in the structural coupling have a similar effect. Fig. 8 shows the resonant amplitude of beam 1 at Ω_r as a function of the stiffness loss ratio for two different structural couplings. As shown in Fig. 8a, for a moderately coupled system ($R = 0.1$), as the stiffness loss decreases, the resonant amplitude of beam 1 at Ω_r increases, which corresponds to the trend shown in Fig. 6. In other words, for a moderately coupled bladed-disk under $\Delta f = -0.08$, the increase in the coupling in the vicinity of $R = 0.1$ results in the increase in the resonant amplitude. Similarly, Fig. 8b shows that under $R = 0.3$ and $\Delta f < -0.08$, the decrease in the stiffness loss ratio $|\Delta f|$ results in the increase in the resonant amplitude, while for $\Delta f > -0.08$, the decrease in the stiffness loss ratio $|\Delta f|$ results in the decrease in the resonant amplitude, which verifies the transition effect observed in Fig. 6.

4.3.3. Effect of engine order

For an undamaged bladed-disk, if the engine order $C \leqslant N/2$, increasing the engine order shifts the resonant peak to a higher frequency region, whereas if $C > N/2$, increasing the engine order decreases the resonance frequency. Increasing C for $C \leqslant N/2$ or decreasing C for $C \geqslant N/2$ also results in the decrease in the amplitude of the resonant peak. These can be readily observed from Eqs. (26) and (27).

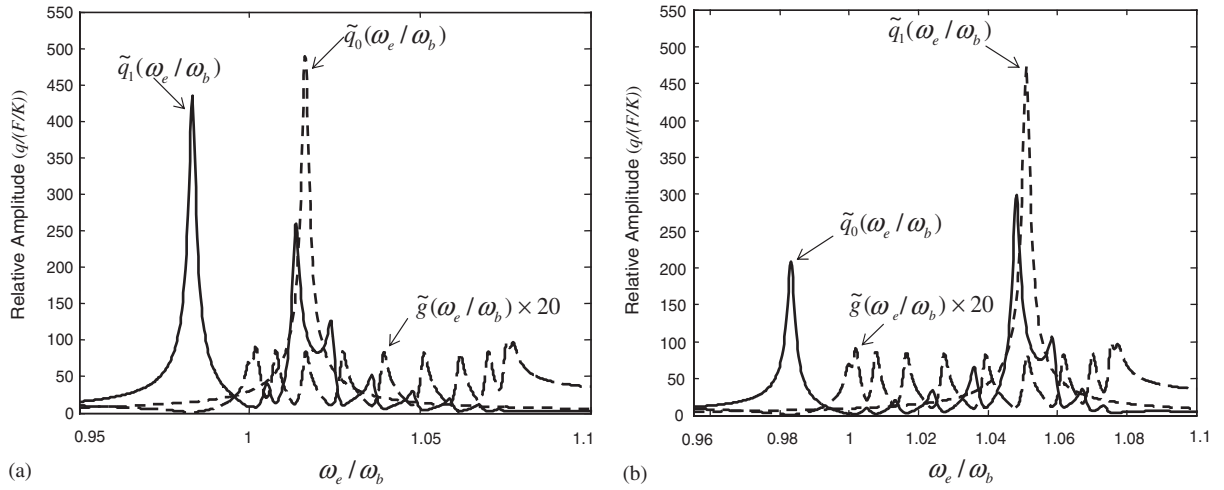

Fig. 9. $\tilde{q}_1(\omega_e/\omega_b)$, $\tilde{q}_0(\omega_e/\omega_b)$ and $\tilde{g}(\omega_e/\omega_b)$ with $N=20$, $R=0.2$, $\Delta f=-0.08$, $\xi=0.001$ for different engine order excitations: (a) $C=3$; (b) $C=6$.

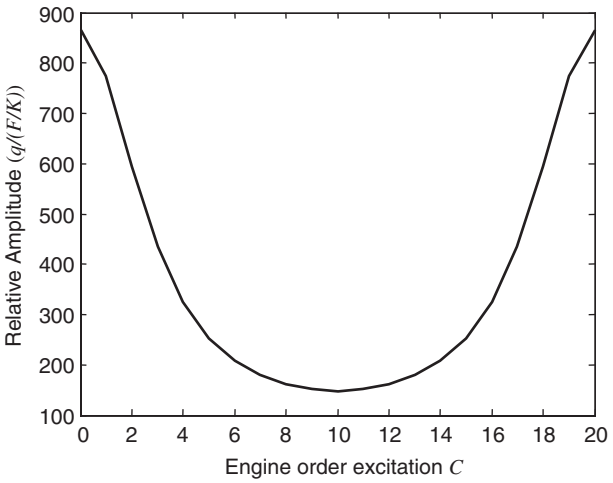

Fig. 10. Amplitude of beam 1 of the damaged structure at excitation frequency Ω_r versus engine order excitation C with $N=20$, $R=0.2$, $\xi=0.001$and $\Delta f=-0.08$.

Fig. 9 exhibits $\tilde{q}_1$, $\tilde{q}_0$, and $\tilde{g}$ under different engine order excitations for beam 1. Compared with that $\tilde{q}_1$ shown in Fig. 4 ($C=0$), when C increases from 0 to 3 or 6, the first resonant amplitude of $\tilde{q}_1$ (at frequency Ω_r) decreases. Eq. (36b) shows that increasing the engine order C for $C\leqslant N/2$ or decreasing C for $C\geqslant N/2$ results in the increase of $[\sqrt{1+(\Delta f/2R^2)^2}-\cos C\sigma]^2$, and the resonant amplitude of beam 1 at Ω_r decreases, which is shown in Fig. 10. Therefore, when $C\neq 0$ or N, the maximum amplitude experienced by beam 1 may not be at frequency Ω_r. Fig. 11 shows that the largest beam amplitude experienced by the damaged bladed-disk for two different engine orders

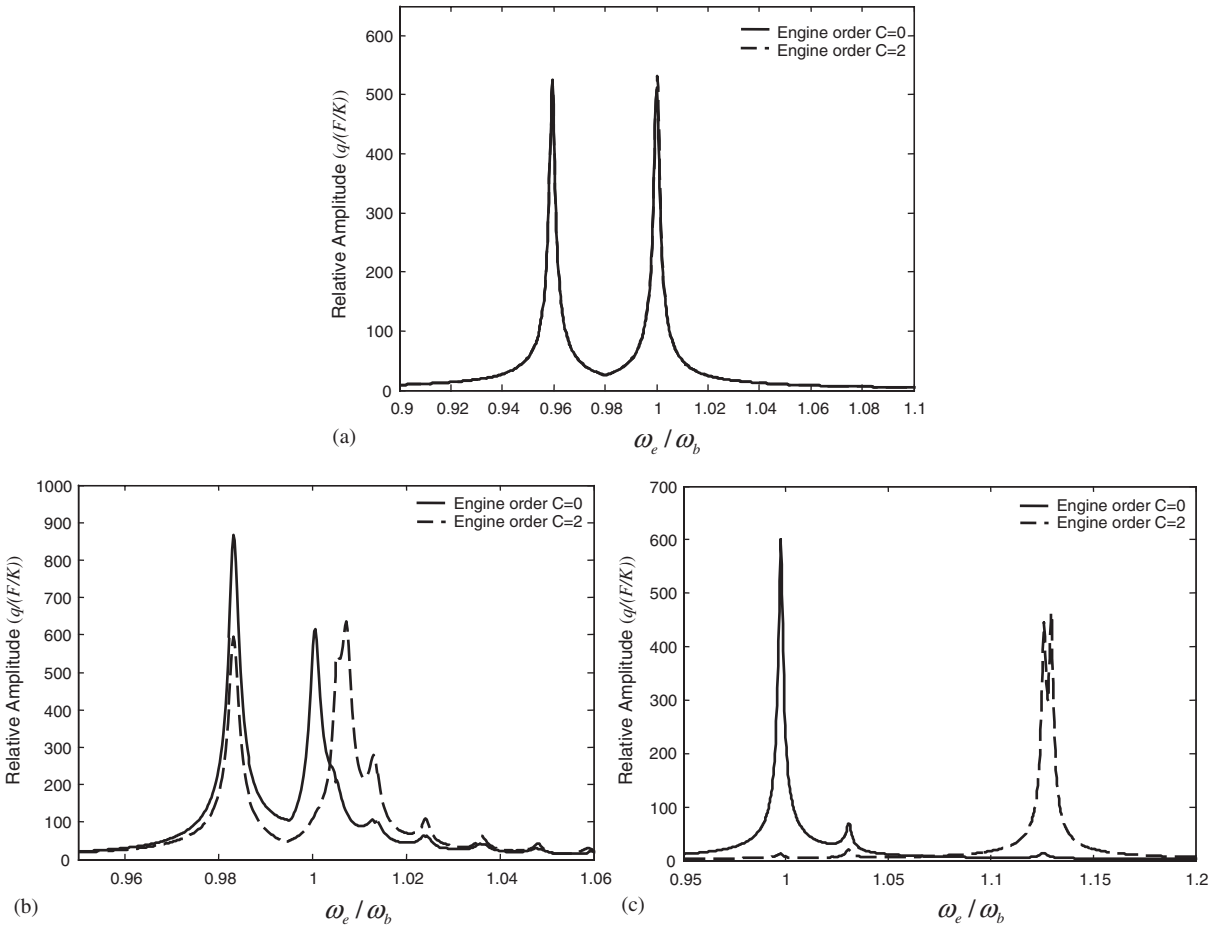

Fig. 11. Largest beam amplitude of damaged structure versus excitation frequency for engine order excitations ($C = 0$ and 2) with $N = 20$, $\xi = 0.001$, and $\Delta f = -0.08$: (a) $R = 0.02$; (b) $R = 0.2$; (c) $R = 0.85$.

($C = 0$ and 2). For a very weakly coupled bladed-disk ($R = 0.02$, $\Delta f = -0.08$) where $|\Delta f/R^2| \gg 1$, it can be observed in Fig. 11a that the engine order has little effect on the response, since the value of $[\sqrt{1 + (\Delta f/2R^2)^2} - \cos C\sigma]^2$ is not significantly affected by the engine order C. With the increase of coupling, the value of $[\sqrt{1 + (\Delta f/2R^2)^2} - \cos C\sigma]^2$ becomes dependent upon the engine order C. For a moderate coupling ($R = 0.2$, $\Delta f = -0.08$), it is shown in Fig. 11b that increasing C from 0 to 2 will decrease the amplitude of the low frequency peak significantly, while the second main peak shifts to a higher frequency region. For a strongly coupled bladed-disk, the value of $[\sqrt{1 + (\Delta f/2R^2)^2} - \cos C\sigma]^2$ increases drastically when C changes from 0 to 2. Hence, the resonant response amplitude of beam 1 at Ω_r is very low as shown in Fig. 11c. It is worth

emphasizing that for a strongly coupled bladed-disk, the effects of engine order excitation on the vibratory behavior of the damaged bladed-disk and on that of the undamaged bladed-disk are similar. One can observe in Fig. 11c that the main peaks of the damaged response are shifted to higher frequencies with decreasing amplitude when C changes from 0 to 2. Fig. 11c also shows that the two main peaks are very close to each other with comparable amplitudes.

4.3.4. Effect of number of blades

Observe Eqs. (22) and (23). Clearly, the response amplitude of the bladed-disk depends upon the number of blades. For a very weakly coupled bladed-disk, (i.e., $R \ll 1$), we have the following approximations:

$$\frac{\Delta f}{N}\sum_{r=1}^{N}\frac{1}{1-\Omega^2+2R^2[1-\cos(r-1)\sigma]+\mathrm{j}\cdot 2\xi\Omega}\approx\frac{\Delta f}{1-\Omega^2+\mathrm{j}\cdot 2\xi\Omega}$$

and

$$\frac{\Delta f}{N}\sum_{r=1}^{N}\frac{\cos(i-1)(r-1)\sigma}{1-\Omega^2+2R^2[1-\cos(r-1)\sigma]+\mathrm{j}\cdot 2\xi\Omega}\approx\frac{\Delta f}{N}\sum_{r=1}^{N}\frac{\cos(i-1)(r-1)\sigma}{1-\Omega^2+\mathrm{j}\cdot 2\xi\Omega}=0.$$

Therefore, if $R \ll 1$, Eqs. (22b) and (23) can be simplified as

$$q_1 \approx \frac{F}{K}\frac{1/\left(1-\Omega^2+2R^2(1-\cos C\sigma)+j\cdot 2\xi\Omega\right)}{1+\left[\Delta f/\left(1-\Omega^2+j\cdot 2\xi\Omega\right)\right]}, \tag{40}$$

and

$$q_i \approx \frac{F}{K}\frac{1}{1-\Omega^2+2R^2(1-\cos\ C\sigma)+j\cdot 2\xi\Omega} \quad (i=2,3,\ldots,N). \tag{41}$$

For illustration purpose, the following results are obtained by direct numerical solution of the damaged response. Fig. 12a shows that the number of blades has little effect on the response for a very weakly coupled damaged structure ($R = 0.02$). This verifies the validity of the approximate analytical solution given in Eqs. (40) and (41). For a moderately coupled bladed-disk ($R = 0.2$), as the number of blades increases from 10 to 20, the first peak's amplitude increases greatly. Meanwhile, the second peak's amplitude also increases, as shown in Fig. 12b. For a strongly coupled bladed-disk ($R = 0.85$), as the number of blades increases, the main peak of the damaged response is shifted to lower frequency region (Fig. 12c). Clearly, the effect of number of blades is more significant for a strongly coupled damaged bladed-disk.

When the number of blades N is small, the amplitude response of a moderately coupled damaged bladed-disk has clear dependence upon N (see Eqs. (22) and (23)). For a sufficiently large N, as shown in Eq. (36b), $[\sqrt{1+(\Delta f/2R^2)^2}-\cos\ C\sigma]^2$ decreases as the number of blades N increases. If $N\to\infty$, the value of $[\sqrt{1+(\Delta f/2R^2)^2}-\cos\ C\sigma]^2$ approaches the minimum, given as $[\sqrt{1+(\Delta f/2R^2)^2}-1]^2$. Therefore, for large N, the resonant amplitude of the cracked blade at frequency Ω_r increases as N increases. Fig. 13 illustrates the effect of number of blades on the resonant amplitude of the cracked blade at Ω_r under moderate coupling. It is shown that when N

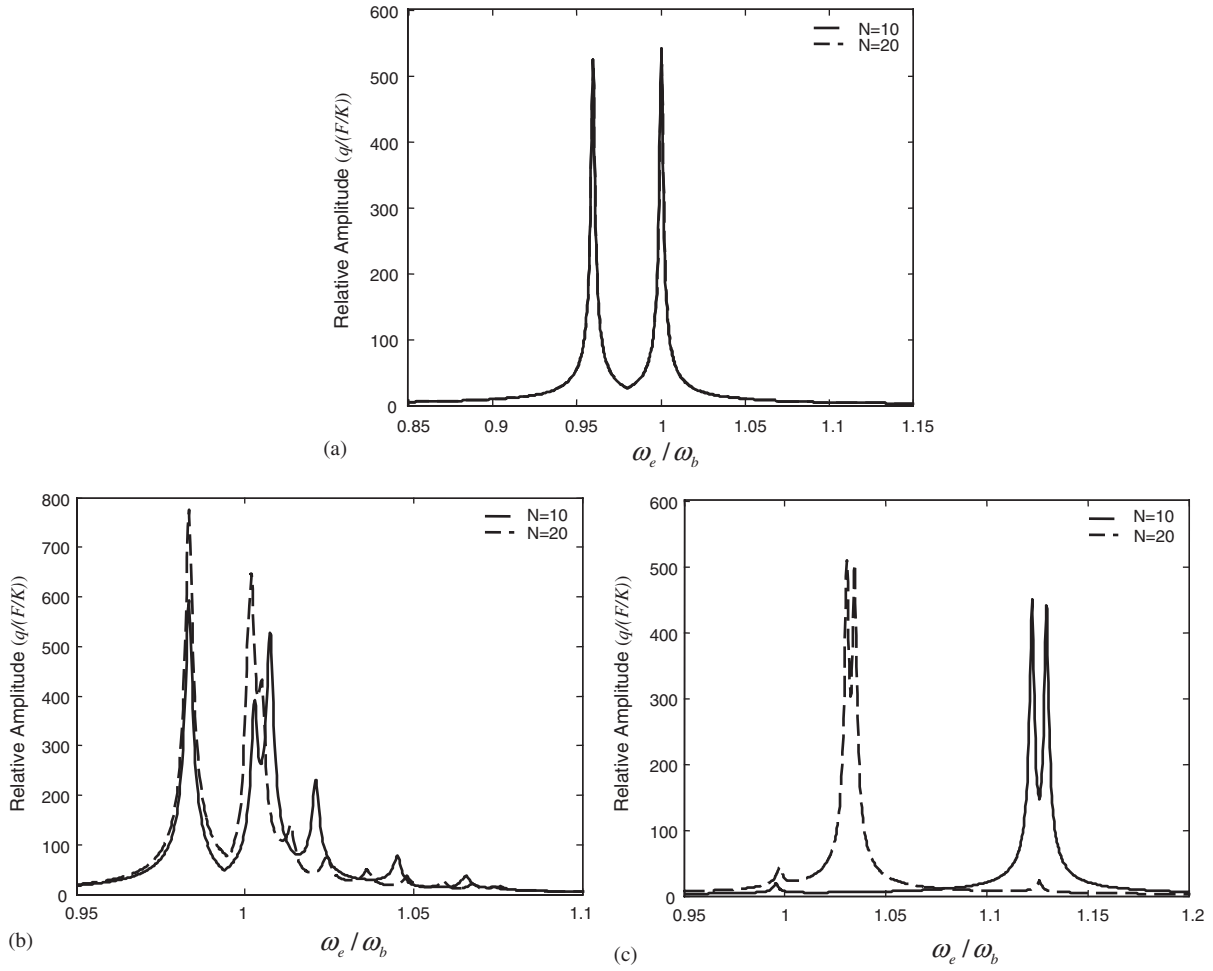

Fig. 12. Largest beam amplitude of damaged structure versus excitation frequency for different numbers of beams ($N = 10$ and 20) with $\xi = 0.001$, $\Delta f = -0.08$, and $C = 1$: (a) $R = 0.02$; (b) $R = 0.2$; (c) $R = 0.85$.

is small, the resonant amplitude changes with the number of blades drastically. When N is large, increasing N leads to the monotonic increase of the resonant amplitude, but the increment becomes smaller and smaller. The reason is obvious: at $\Omega = \Omega_r$ the bladed-disk experiences vibration localization and thus with N increasing it is more and more difficult for the vibration energy to be propagated throughout the entire structure.

5. Concluding remarks

In this research, we carry out a systematic analysis to evaluate the crack effect on the vibratory response of a simplified bladed-disk model. A fracture mechanics based approach is employed to

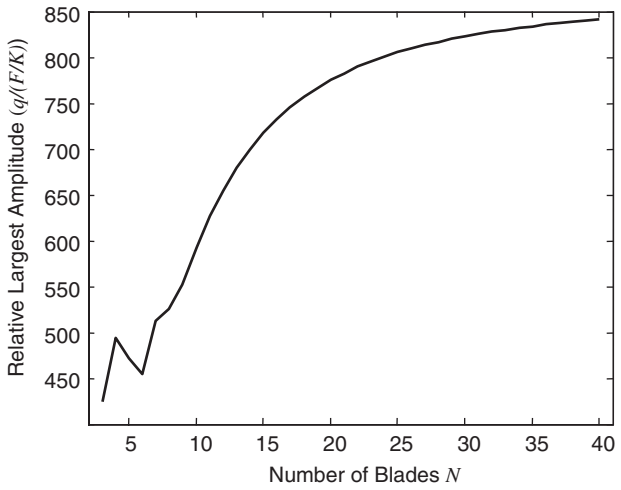

Fig. 13. Resonant amplitude of beam 1 at Ω_r for the damaged structure versus number of beams with $R = 0.2$, $\xi = 0.001$, $\Delta f = -0.08$, and $C = 1$.

evaluate the stiffness loss, and analytical solutions to the free and forced responses of the bladed-disk are developed. It is found that even a small crack damage could cause vibration mode localization and forced response localization. We have explored the intrinsic relations between the response amplitudes and various system parameters such as internal coupling, crack severity, excitation patterns, and number of blades systemically. Qualitative and quantitative conclusions are obtained, by correlated analytical and numerical studies. These conclusions could be used in the evaluation of crack effect and also could provide guidelines in structural health monitoring.

References

[1] S.S. Mester, H. Benaroya, Periodic and near-periodic structures, *Shock and Vibration* 2 (1) (1995) 69–95.
[2] J.C. Slater, G.R. Minkiewicz, A.J. Blair, Forced response of bladed disk assemblies—a survey, *The Shock and Vibration Digest* 31 (1) (1999) 17–24.
[3] C. Pierre, M.P. Castanier, W.J. Chen, Wave localization in multi-coupled periodic structures: application to truss beams, *ASME Applied Mechanics Review* 49 (2) (1996) 65–86.
[4] C.H. Hodges, Confinement of vibration by structural irregularity, *Journal of Sound and Vibration* 82 (3) (1982) 411–424.
[5] C. Pierre, E.H. Dowell, Localization of vibrations by structural irregularity, *Journal of Sound and Vibration* 114 (1987) 549–564.
[6] S.-T. Wei, C. Pierre, Localization phenomena in mistuned assemblies with cyclic symmetry part I: free vibrations; part II: forced vibrations, *ASME Journal of Vibration, Acoustics, Stress and Reliability in Design* 110 (1988) 429–449.
[7] M.P. Castanier, C. Pierre, Lyapunov exponents and localization phenomena in multi-coupled nearly periodic systems, *Journal of Sound and Vibration* 183 (3) (1995) 493–515.

[8] M.-T. Yang, J.H. Griffin, A reduced order approach for the vibration of mistuned bladed disk assemblies, *ASME Journal of Engineering for Gas Turbines and Power* 119 (1) (1997) 161–167.
[9] M.P. Mignolet, W. Hu, Direct prediction of the effects of mistuning on the forced response of bladed disks, *ASME Journal of Engineering for Gas Turbines and Power* 120 (1998) 626–634.
[10] R. Bladh, M.P. Castanier, C. Pierre, Reduced order modeling and vibration analysis of mistuned bladed disk assemblies with shrouds, *ASME Journal of Engineering for Gas Turbine and Power* 121 (1999) 515–522.
[11] C.W. Cai, Y.K. Cheung, H.C. Chan, Mode localization phenomena in nearly periodic system, *Journal of Applied Mechanics* 62 (1995) 141–149.
[12] W.-C. Xie, S.T. Ariaratnam, Vibration mode localization in disordered cyclic structures, I: single substructure mode, *Journal of Sound and Vibration* 189 (1996) 625–645.
[13] J.-T. Kim, N. Stubbs, Crack detection in beam-type structures using frequency, *Journal of Sound and Vibration* 259 (1) (2003) 145–160.
[14] P. Gudmunson, Eigenfrequency changes of structures due to cracks, notches or other geometrical changes, *Journal of the Mechanics and Physics of Solids* 30 (1982) 339–353.
[15] J.M. Barsom, S.T. Rolfe, *Fracture and Fatigue Control in Structures: Applications of Fracture Mechanics*, Prentice-Hall, West Conshohoken, PA, 1999.
[16] D.J. Mead, Wave propagation and natural modes in periodic systems: I. mono-coupled systems, *Journal of Sound and Vibration* 40 (1975) 1–18.